Int. J. Heat Mass Transfer. Vol. 23, pp. 1055–1068
Pergamon Press Ltd. 1980. Printed in Great Britain

CONVECTIVE HEAT TRANSFER ON A PLATE IN AN IMPINGING ROUND HOT GAS JET OF LOW REYNOLDS NUMBER

CZ. O. POPIEL,* TH. H. VAN DER MEER and C. J. HOOGENDOORN
Delft University of Technology, The Netherlands

(*Received* 4 *December* 1978 *and in revised form* 14 *November* 1979)

Abstract—An experimental study has been made of the local heat transfer on the plane isothermal surface in the normal impinging round hot jet of combustion products produced by a rapid heating tunnel burner. A conductivity heat plug, impact tubes and fine wire thermocouples were used to measure heat flux, mean velocity and temperature distributions. Some centerline relative turbulence intensity measurements were done with a Laser Doppler Anemometer. All measurements were obtained at two efflux Reynolds numbers 1860 and 1050; the density ratio between hot combustion products and ambient air was 7.6. Heat transfer was measured at distances between 2 and 20 D. The stagnation point heat transfer within the distances $x/D \leqslant 5$ is in good agreement with Sibulkin's laminar boundary layer theory. In the developed region $x/D \geqslant 8$ strong free jet turbulence effects augmenting the convective heat transfer were observed. The radial heat transfer distributions are qualitatively consistent with those known in the impinging cold jet investigations at low Reynolds numbers.

NOMENCLATURE

c_p, specific heat at constant pressure [J kg^{-1} K];
D, burner nozzle diameter [m];
D_e, equivalent diameter, $D(\rho_j/\rho_a)^{1/2}$ [m];
h, enthalpy [J kg^{-1}];
h_R, reference enthalpy, $\frac{1}{2}(h_{rx} + h_w)$ [J kg^{-1}];
k, thermal conductivity [W m^{-1} K^{-1}];
L, length of the copper rod [m];
Nu, Nusselt number, $\alpha D/k$;
p, pressure [N m^{-2}];
Δp, impact tube response [N m^{-2}];
q, heat flux density [W m^{-2}];
Pr, Prandtl number;
r, radius [m];
$r_{1/2}$, radius at which a measured value reaches one half of its maximum value [m];
Re, collision Reynolds number, $U_x D/\nu$;
Re_0 outlet (efflux) Reynolds number, $U_0 D/\nu_0$;
t', fluctuating component of temperature [K];
T, time average temperature [°C];
ΔT_0, temperature difference, $T_0 - T_a$ [K];
ΔT_x, temperature difference, $T_x - T_a$ [K];
Tu, relative turbulent intensity, $100(\overline{u'^2})^{1/2}/U$ [%];
u', fluctuating component of axial velocity [m s^{-1}];
U, time average axial velocity [m s^{-1}];
V, time average radial velocity [m s^{-1}];
x, distance measured from the nozzle [m];
x_0, distance of the virtual jet source from the nozzle [m];

Greek symbols

α, heat-transfer coefficient, $qc_p/(h_{rx} - h_w)$ [W m^{-2} K^{-1}];
β, velocity gradient in radial direction outside of the boundary layer, in the stagnation point vicinity, $(\partial V/\partial r)_{r\to 0}$ [s^{-1}];
ν, kinematic viscosity [m^2 s^{-1}];
ρ, mass density [kg m^{-3}].

Subscripts

a, ambient air;
rx, at radius r and distance x;
x, at radius $r = 0$ and distance x;
o, at the outlet (efflux) section of the nozzle;
w, on the surface of the plate.

1. INTRODUCTION

MANY INDUSTRIAL heating operations (i.e. in the steel and glass industry) now take advantage of the high rates of energy transfer which are obtained with the use of impinging jets. For instance, heat transfer in conventional industrial furnaces occur mostly by thermal radiation. In modern 'rapid heating' furnaces flames and hot combustion products impinge directly on the surface of the solid stock and heat mainly by convection at extremely high heat fluxes. These 'convective furnaces' have many advantages over those where the heat transfer is by radiation (shorter heating-up periods, smaller sizes and lower thermal inertia).

Many process heating systems utilize tunnel burners which produce high velocity jets of completely combusted products. The efficiency of the impinging heating technique creates interest in the convective heat transfer of impinging hot gas jets. It is apparent that ability to predict accurately the distributions of

* Present address: Heat Transfer Section, Technical University. 60965 Poznań, ul. Piotrowo 3, Poland.

the heat transfer rates on the surface in the impingement hot gas jets is necessary, particularly in the optimization of existing processes and in the evaluation of new applications.

In the rapid heating tunnel burners usually the combustion is virtually complete within the tunnel with the minimum local value of the completeness of combustion of 98 per cent [1]. Therefore at the burner mouth we practically have to deal with a hot jet of combustion products. The biggest industrial tunnel burners produce hot jets with an efflux Reynolds number of about 60000 and small ones provide jets with minimum Reynolds numbers below 2000. The impinging jet contains three separate regions, namely the free jet, the stagnation point and the wall jet region. The initial conditions at the outlet section (velocity, temperature and turbulence profiles) influence the flow pattern in the free jet region. And this flow pattern subsequently creates boundary conditions for the flow in the stagnation point region. Only in the wall jet region does the previous history of the jet not influence the flow structure.

Impinging jets have been extensively investigated during the last two decades. Very recently Martin [2] gave a comprehensive survey of literature which is mainly devoted to the heat and mass transfer in impinging cold gas jets. In spite of the large amount of work, both experimental and theoretical, that has been done on heat and mass transfer between flat plates and impinging jets the local heat transfer distribution in many cases can only be approximated very roughly. One of the first papers on impinging heat transfer [3] describes very limited results of measurements of the heat transfer from a hot air jet at temperature differences of up to 400°C and velocities of up to 76 m s^{-1}. A high enthalpy arc-heated nitrogen jet of 5000°K impinging normally on a flat plate in ambient air was investigated by Comfort *et al.* [4]. The heat flux measurements were performed at distances of the plate from the nozzle higher than the core length and at the outlet Reynolds number of about 10^4. In the developed region of the jet their stagnation point heat flux distribution was almost three times higher than the Fay and Riddell laminar boundary layer theory [5]. The impinging heat transfer to a plate from the hot gas jet produced by rapid heating tunnel burners was the subject of theoretical calculations [6] and experimental investigations [1], which were not quite complete.

No known experimental work has been reported about the local heat transfer distributions on the plane surface in an impinging hot gas jet at very low Reynolds numbers and small distances from the nozzle. Evolutions of the velocity, temperature and turbulence in the initial part of the free hot jet region are very roughly known too. The purpose of the experimental study reported in this paper was to fill up some gaps in our knowledge about the heat transfer in impinging hot gas jets, providing both practical data for engineers and reliable experimental information which is required to validate the laminar flow theory and the numerical procedures using mathematical models of turbulence.

2. EXPERIMENTAL SET-UP AND MEASURING EQUIPMENT

Figure 1 illustrates schematically the main parts of the employed instrumentation. The round jet of hot combustion products impinged normally on a horizontal intensely water cooled isothermal plate in which heat flux meters and a static pressure meter were inserted. The tunnel burner was attached to an X–Y–Z positioner which was operated manually. The locations of the burner vs. the meters in the plate or the locations of the velocity and temperature probes vs. the burner were recorded with the traversing system [7]. The traversing system consisted of the X–Y–Z positioner, three two-photodiode displacement transducers and a sweep drive unit (digit-voltage converter). This arrangement allowed for direct plotting of the heat flux, static pressure, velocity and temperature distributions on an X–Y recorder. For all these measurements the position of the jet axis was found from the radial distributions of measured values. The mean velocity, temperature, static pressure, heat flux and turbulence intensity were measured in separate runs at constant readings of the rotameters for a fixed Reynolds number.

Isothermal plate

The isothermal plate (573 × 320 mm) was made of copper in order to suppress lateral temperature differences within it. The outer surface of the plate was polished and its temperature was controlled by 8 Cu-Constantan thermocouples and kept at fixed level (above the dew point). The temperature of cooling water was maintained automatically at a constant value with two thermostats. In the plate two heat flux meters (see Fig. 2) and a static pressure transducer with a hole of 0.5 mm diam. were built in.

Tunnel burner

A small industrial rapid heating tunnel burner was used as a source of a premixed flame jet which could be treated as a hot gas jet. In the original version this burner has a tangential inlet of the gas–air mixture producing a swirl as a flame holder and allowing external ignition. In order to obtain a jet without swirl the tangential connection was replaced by an axisymmetric connection. Furthermore a small disk flame holder was used in the improved version of the burner as shown in Fig. 3.

Dutch Groningen natural gas [8] was used as fuel with the following characteristics for a stoichiometric ratio and dry air.

Composition (in % by vol.): $CH_4 = 81.3$, $C_2H_6 = 2.85$, $C_mH_n = 0.60$, $CO_2 = 0.89$, $N_2 = 14.35$, $O_2 = 0.01$.

Molecular mass: 18.36 [kg kmol^{-1}].

Net caloric value: 31650 [kJ nm^{-3}].

Air/fuel ratio: 8.407 [m^3 air:m^3 gas].

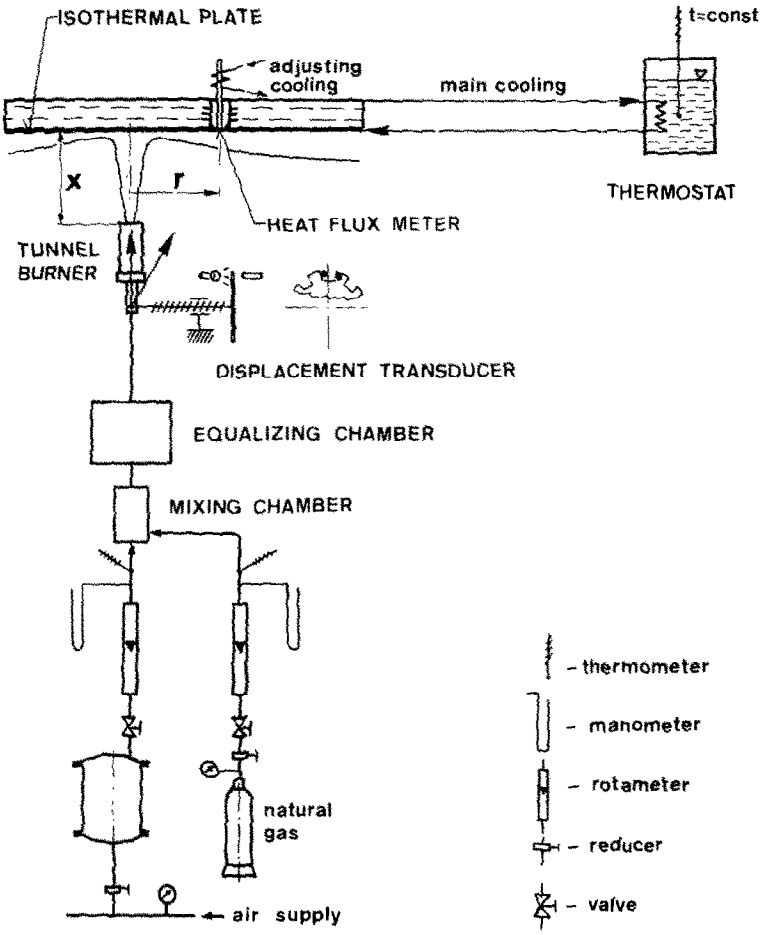

FIG. 1. Experimental apparatus.

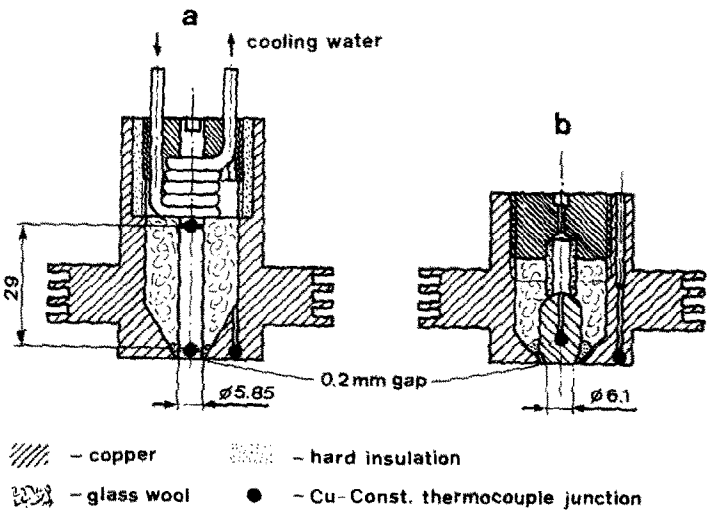

FIG. 2. Heat flux meters: (a) conductivity plug; (b) α-calorimeter.

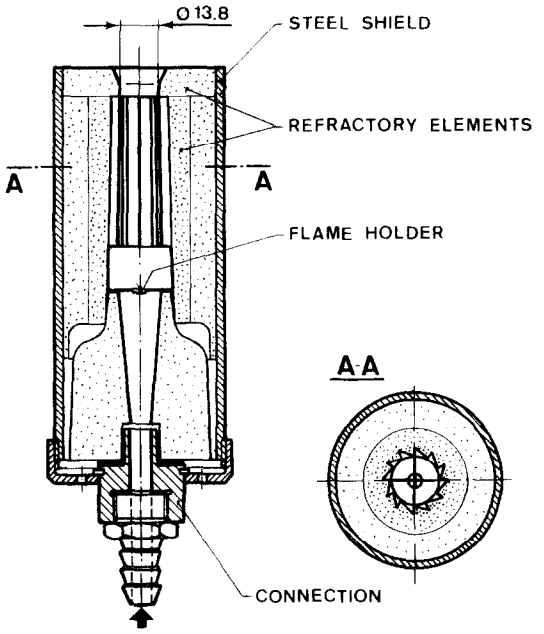

FIG. 3. Rapid heating tunnel burner.

Combustion products/fuel ratio: 9.43 [m^3 fume:m^3 gas].

Composition of combustion products (in % by vol.): $CO_2 = 9.56$, $N_2 = 72$, $H_2O = 18.44$.

Molecular mass of combustion products: 27.69 [$kg\,kmol^{-1}$].

Adiabatic flame temperature: 1860°C.

The concentration of the gas–air mixture was stoichiometric. Dry air was delivered by an air pressure line. The gas was available from bottles. The standard flow volumes of gas and air were adjusted by means of rotameters then mixed in a mixing chamber and after a settling chamber guided to the burner.

Heat flux meters

All measurements of the heat flux distributions were carried out with the conductivity plug-type heat flux meter (Fig. 2a). The front of the copper rod was situated flush with the surface exposed to the impinging hot gas jet. The temperature drop on the isolated part of the rod was measured with a Cu-Constantan differential thermocouple of 0.1 mm diam. mounted in holes of 0.4 diam. The heat flux conducted through the rod was removed by cooling water. The temperature of the front of the rod was maintained at the same temperature as its surrounding surface exposed to the impinging jet, by adjusting the water cooling of the rod. In this way we could obtain an isothermal heat transfer surface and prevent heat losses from the rod to its surroundings. The response of the differential thermocouple (ΔE) was almost proportional to the heat flux value:

$$q = \frac{k(T)}{L}\frac{\Delta E}{C(T)} \qquad (1)$$

and only small corrections of the conductivity of the copper rod $k(T)$ and the thermocouple constant $C(T)$ due to the different temperature drops were taken into account. An X–Y recorder registered the output of the heat flow meter as a function of the displacement of the burner. The second heat flux meter (Fig. 2b) based on a transient method described in [9] did not require a calibration and was used for the initial testing of the first probe.

Temperature probe

Mean temperatures of the hot gas jet were measured using two kinds of fine wire thermocouples (Pt–10% RhPt and 6% RhPt – 30% RhPt) varying in dia. from 180 to 50 μm [10]. The bare thermocouple wires were butt-welded. Afterwards the fine junction wires were butt-welded to the tops of thicker wires of the same material and coated with a non-catalytic layer of a mixture of berylium oxide and yttrium chloride [11]. These supporting prongs protruded from an inconel shield of a mantle thermocouple lead. Such sensors could be inserted in the water-cooled jacket of a thermocouple support (Fig. 4). The radiation effect was evaluated using the extrapolation technique which consists in the comparison of the responses obtained from the thermocouple sensors with different junction diameters (Fig. 5).

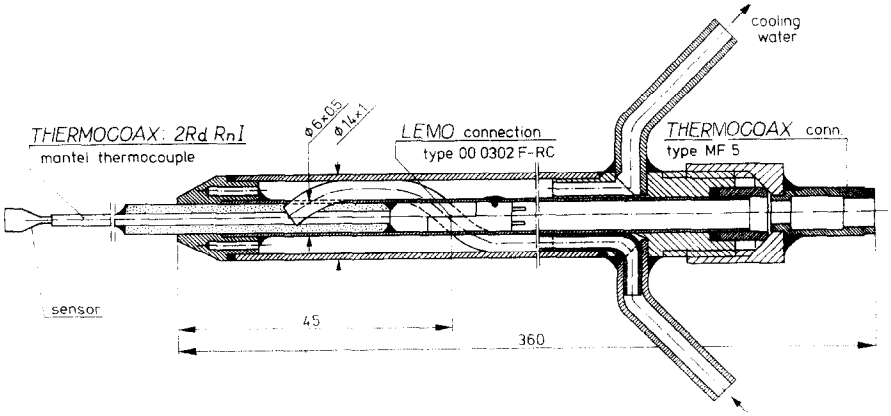

FIG. 4. Miniature thermocouple support with sensor.

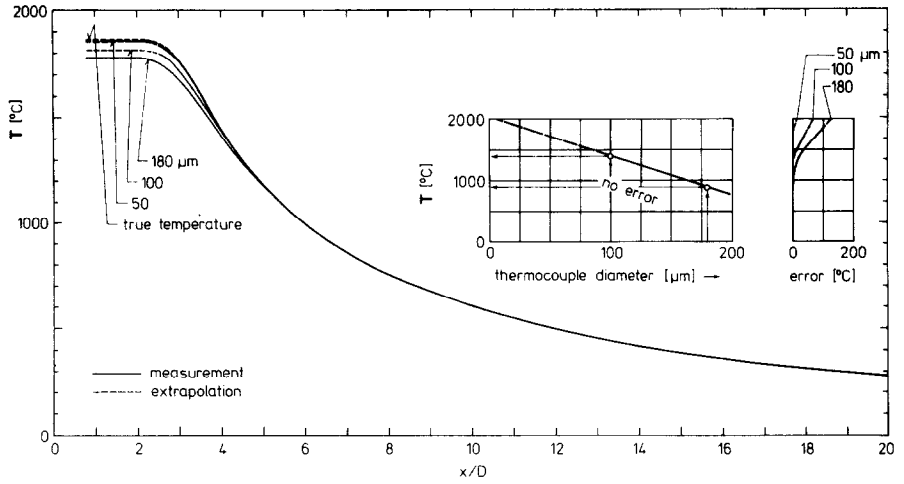

FIG. 5. Axial distribution of the temperature (for $Re_o = 1860$).

Velocity measurements

Most mean velocity measurements were carried out using a total head Pitot tube. A sharp ended impact tube with a thin-walled squarely truncated hollow cylinder probe tip geometry (of 1.2/0.8 mm in diam. and 12 mm in length) was used. This shape is most suitable for measurements in hot gases because the effects of simultaneous longitudinal velocity and temperature fluctuations on a reading of the total head tube are in opposite directions [12]:

$$\Delta p = \tfrac{1}{2}\bar{\rho}U^2\left(1 + \frac{\overline{u'^2}}{U^2} - 2\frac{\overline{u't'}}{U\,T[\mathrm{K}]}\right) \qquad (2)$$

where: $t'/T = t'T^{-1} = -\rho'/\bar{\rho}$. Becker and Brown [13] used the difference between the responses of a sharp ended and a sphere-nosed impact tubes as a differential Pitot tube for lateral turbulence intensity measurements. Unfortunately in our case it was impossible to notice this pressure difference.

The small probe tips exposed to the high temperature gas jet were made of molybdenum and pressed into the water-cooled copper supports. For direct velocity and static pressure measurements with the X–Y recorder a Furness Controls micromanometer was used with a maximum sensitivity of 0.005 mm H_2O.

Some axial average velocity and turbulence intensity measurements were made with a Laser Doppler Anemometer (LDA) working in the interference fringe mode. The 5 mW He–Ne laser beam was split and preshifted by a rotating grating. The fringe spacing was 5.7 μm thus the measuring volume of 0.12 mm in dia. and 2.2 mm in length contained 21.8 fringes. A photomultiplier detected the scattered light from particles crossing the measuring volume. The MgO particles were generated by a vertically shaking strainer situated directly before the burner. The signal from the photomultiplier was analysed by a spectrum analyser and a signal processing counter to determine the velocity and turbulence intensity.

3. RESULTS

Flow structure

Figure 6 shows the centerline velocity distribution for the jets with various density ratios of the fluids in an ambient environment and in the jet. These distributions can be described with one equation using the equivalent diameter $D_e = D(\rho_0/\rho_a)^{1/2}$ which is based on the assumption that the development of the jet is determined by the total jet momentum [20]:

$$U_o/U_x = 6.4\,D_e/(x + x_o) \qquad (3)$$

where x is the distance of the virtual jet source from the nozzle.

Beyond the distance of about $x = 35D_e$ for the hot jet with the efflux Reynolds number of $Re_o = 1050$ and density ratio $\rho_a/\rho_o = 7.6$ we can notice the effect of buoyancy which according to Chen and Rodi [21] can be expected approximately at the distances

$$(x/D_e)_{\text{buoyancy effect}} \geq 0.5\,F^{1/2}(\rho_a/\rho_o)^{1/4}$$

where: $F = \rho_o U_o/g(\rho_a - \rho_o)D$ – Froude number. In our case we have $(x/D_e)_{b.\,\text{eff.}} = 26.7$. The small deviation of Wygnanski and Fiedler's [14] data at higher distances could be caused by an effect of surrounding walls even though they were made of mesh screens.

The axial distributions of the relative turbulence intensity and average velocity obtained with the LDA technique are presented in Fig. 7. Very near to the outlet section the turbulence levels of the cold and hot jets are almost the same ($Tu_o = 6$ to 7 per cent) which proves that the initial turbulence is mainly determined by the geometry of the outlet part of the tunnel burner. Further along the jet axis we observe a rapid rise in turbulence which is coming from the mixing region and is more pronounced in the hot jet than in the cold

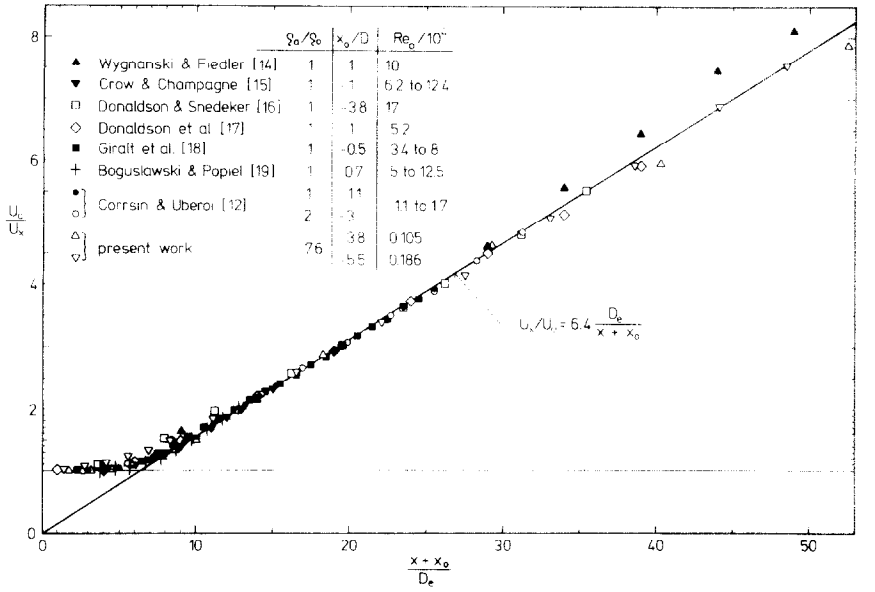

FIG. 6. Centerline velocity decay.

one. The maximum of the turbulence at the distance $x \simeq 6D$ probably is formed by the eddies of the possible ordered structure of the free jet. The influence of the density ratio on the centerline temperature decay is shown in Fig. 8. Our results and those reported by Corrsin and Uberoi [12] do not obey the temperature decay relationships proposed in [22 and 23] using the equivalent diameter.

The velocity spread for the free hot jet within the distance $x/D = 5$ to 17 is shown in Fig. 9 and can be characterized by the equation

$$r_{1/2} = 0.093\ (x + x_0), \text{ where } x_0 = 1D \qquad (4)$$

which for long distances tends to the formula describing the spread of an isothermal jet investigated by Donaldson *et al.* [17]. The bigger spread of temperature is noticeable due to a stronger turbulent transport mechanism of the scalar quantity.

The evolutions of the radial profiles of the velocity and temperature are shown in Fig. 10. The velocity and temperature distributions at the outlet section are very close to uniform profiles. Figure 11 shows a decay of a maximum temperature in the wall jet region of the impinging hot jet. The slight deviation of our results from those obtained by Era and Saima [24] must have been caused by the difference of the Reynolds number and the lower temperature difference ($T_0 - T_a \lesssim 200°C$).

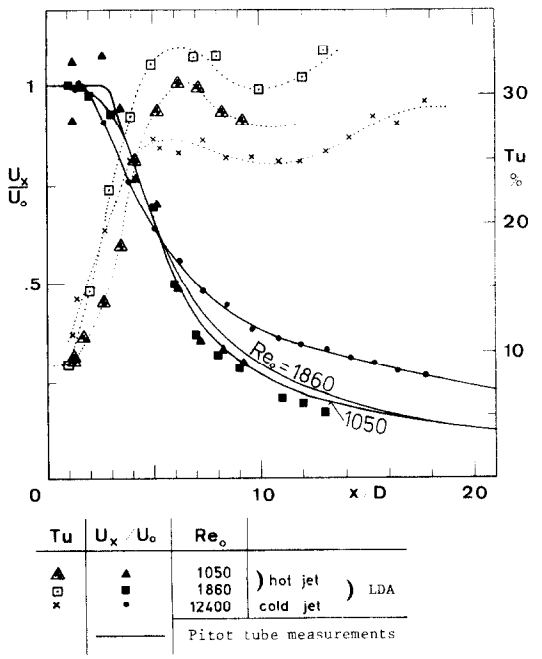

FIG. 7. Axial relative turbulence intensity and mean velocity distributions along the axis.

Heat transfer at the stagnation point

The Nusselt numbers were obtained with the formula:

$$Nu = \frac{qc_pD}{(h_x - h_w)k} \qquad (5)$$

The physical properties were determined for the reference enthalpy h_R recommended by Eckert and Drake [25] and taken from [8]. The radiation heat transfer between the outlet area of the burner and the plate for short distances did not exceed 5 per cent and was neglected.

The axial variations of the heat transfer rates at the stagnation point are shown in Fig. 12. A similar behaviour of these results is found in the cold impinging jet experiments of Gordon and Cobonque [26] performed at higher Reynolds numbers ($Re_o \geq 7000$).

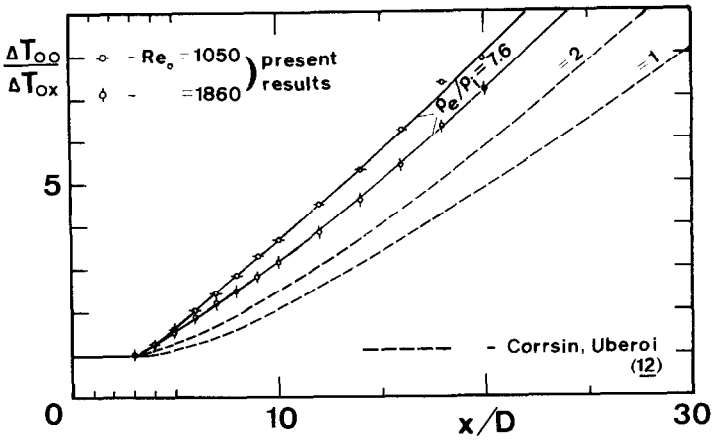

FIG. 8. Centerline temperature decay.

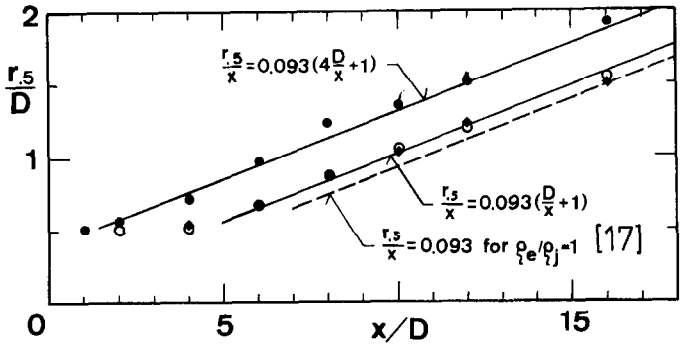

FIG. 9. Hot jet spread for $\rho_a/\rho_o = 7.6$ and 1860: ○—half velocity radius; ◇—half static pressure (on the plate in the impinging hot jet); ●—half temperature radius; - - -—half velocity radius for isothermal jet [17].

The correlation equations and experimental data are presented in Figs. 13 and 14. The first diagram shows that the equation

$$Nu = \left(0.65 + 0.084\frac{x}{D}\right) Re^{0.5}\, Pr^{0.4} \qquad (6)$$

represents very well the experimental results within the distance $2 \leq x/D \leq 5$. In this region the heat transfer rates increase with an increasing distance. Above $x = 10\,D$ we have the developed turbulent heat transfer region in which the equation

$$Nu = \left(137 - 1.8\frac{x}{D}\right) 10^{-3}\, Re^{0.75}\, Pr^{0.4} \qquad (7)$$

describes the experimental results (Fig. 14). The presence of these two domains with the same effect of Reynolds numbers has been found by Coeuret [28] using an electrochemical method in liquid and a pipe as a nozzle.

In order to determine the heat transfer at the stagnation point on the plate in an impinging jet using the laminar boundary layer solution given by Sibulkin [29]

$$Nu = 0.763\,(\beta D/U_x)^{0.5}\, Re^{0.5}\, Pr^{0.4} \qquad (8)$$

the local radial velocity gradient $\beta = (\partial V/\partial r)_{r\to 0}$ must be evaluated, where V is the radial velocity outside of the boundary layer. This can be done experimentally by measuring the static pressure distribution on the surface in the immediate vicinity of the stagnation point [4 and 16]. Assuming the flow outside the boundary layer to be locally incompressible, we have

$$V = \sqrt{\left[\frac{2(p_x - p_{rx})_w}{\rho}\right]} \qquad (9)$$

where p_{rx} and p_x are the static pressures measured on the plate surface at the radius r (which is measured from the stagnation point along the plate surface) and at the stagnation point ($r = 0$) respectively. As the velocity distribution along the plate is assumed to have the form $V = \beta r(1 + Cr)$ and when the value V/r is plotted against r, the measured points of V/r lie on a straight line and the value of $(V/r)_{r=0}$ is the desired stagnation point radial velocity gradient β.

The tangential (radial) velocity gradient at the stagnation point on the surface of blunt axisymmetric bodies in a uniform cross flow is constant and equal, for instance:

for a cylinder: $\beta = 4U/D$

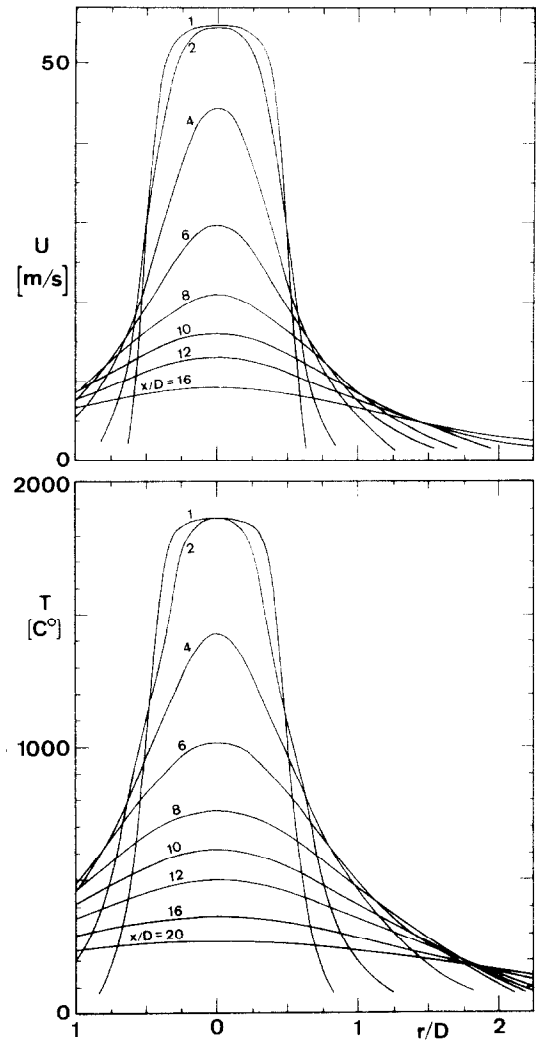

FIG. 10. Radial profiles of velocity and temperature of the hot free jet (for $Re_0 = 1860$ and ρ_a/ρ_e)

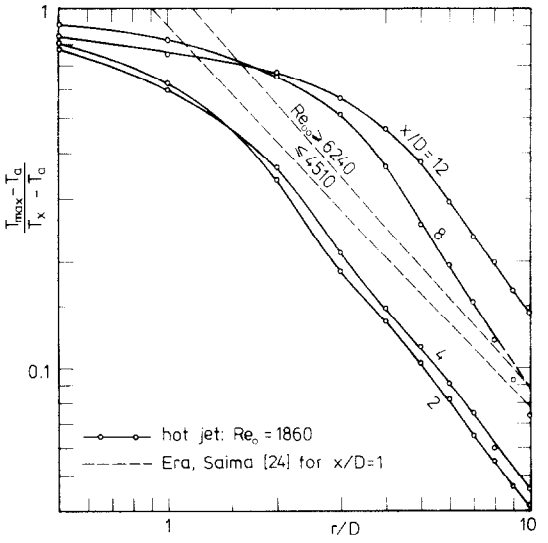

FIG. 11. Decay of maximum temperature in wall jet region of the impinging hot jet.

for a sphere: $\beta = 3U/D$
for a disk [30]: $\beta = U/D$

where U is the velocity of the free stream and D is the diameter of the body. But for the real impinging free jets it is obvious that the change in the collision velocity radial profile $U(r)$ changes the radial velocity gradient β, which is rising in the core region of the jet with a flat efflux velocity profile and is decreasing at the distance beyond the core length when the plate is removed. Only at very small distances between a nozzle and surface which is normally impinged by the jet having a flat efflux velocity profile we can expect that $\beta = \text{constant} \times U_p/D$, which was confirmed by the cold jet measurements of Donaldson *et al.* [17, p. 304]. In the region $x/D \leq 0.5$ (core length) they have obtained $\beta = 0.9\, U_0/D$. The maximum of the β-value localizes itself at the distance where the velocity radial profile is very sharp (approximately immediately after the end of the jet core).

The plot of the heat transfer rates calculated from equation (8) and measured values of β are shown in Fig. 13 as a solid line with black squares. We see that at the distance $x/D \leq 4$ the results of calculations are in an excellent accordance with the direct heat transfer measurements. This means that at the stagnation point, for small distances, due to the strong stabilizing effect of acceleration we have a laminar boundary layer. It is very interesting to notice that the very recently published experimental mass transfer data by Giralt *et al.* [18] (for Schmidt number $Sc = 2.45$) are very consistent with our results. The 10 per cent parallel downward shift of their results at the laminar stagnation point region could be caused by a different initial flow structure of the jet as well as by systematic measurement errors. The longer laminar stagnation point region and the higher maximum in the mass transfer investigation are connected with the longer core length of the isothermal jet used in the mass transfer measurements.

At the distance $x/D = 5$–6 the heat transfer rates reach maxima and turbulence is still growing (see Fig. 7). In this situation the direct effect of turbulence on the heat transfer at the stagnation point starts to become noticeable. In the region $x/D \geq 8$, instead of the direct measured values of β we can also use the generalized impinging jet flow data. From our measurements (for $x/D = 8$ to 20) and those of Comfort *et al.* [4] we have

$$\beta = 0.90\, U_x/r_{1/2}. \tag{10}$$

Using this expression and equation (4) the formula (8) yields

$$Nu = 2.37\left(\frac{x + x_0}{D}\right)^{0.5} Re^{0.5}\, Pr^{0.4} \tag{11}$$

which is valid for the range $x/D = 8$ to 20. The above formula is represented in Fig. 13 by a dashed curve and indeed for larger distances ($x/D \geq 8$) gives the same

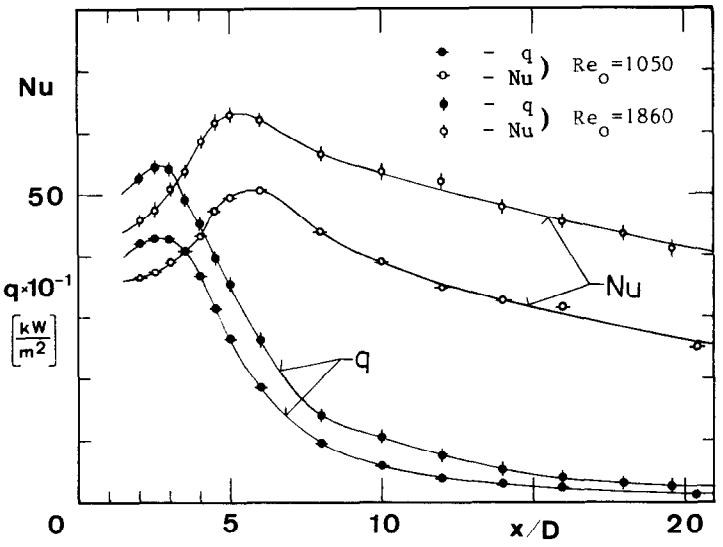

FIG. 12. Heat flux density and Nusselt number distributions at the stagnation point.

results as the Sibulkin's solution using direct measured values of β. It is also interesting to point out that equation (11) is in very good accordance with the results of a numerical calculation obtained by Saad *et al.* [27] for the distance $x/D = 8$. As expected in this region the experimental points lie higher because of the contribution of free jet turbulence transport phenomena.

As the impinging cold jet investigations [17 and 31] have shown, in the region of the well established turbulence effect the heat transfer at the stagnation point can be described by the laminar stagnation point heat transfer rate and a turbulent correction factor which is a function of the free jet turbulence intensity and the collision Reynolds number. Superimposing the results of the laminar boundary layer solution and a turbulence addition recommended by Sikmanovic *et al.* [32] we have:

$$Nu/Re^{1/2} = a\,Pr^{0.4} + b\left(\frac{Tu\,Re^{1/2}}{100}\right) + c\left(\frac{Tu\,Re^{1/2}}{100}\right)^2 \tag{12}$$

where: a in our case is not constant and means the laminar value of $Nu/Re^{1/2}\,Pr^{0.4}$ for $Tu = 0$ (solid line with black squares in Fig. 13) and $b = 1.94, c = -2.41$ are the constants obtained by Sikmanovic *et al.* for the

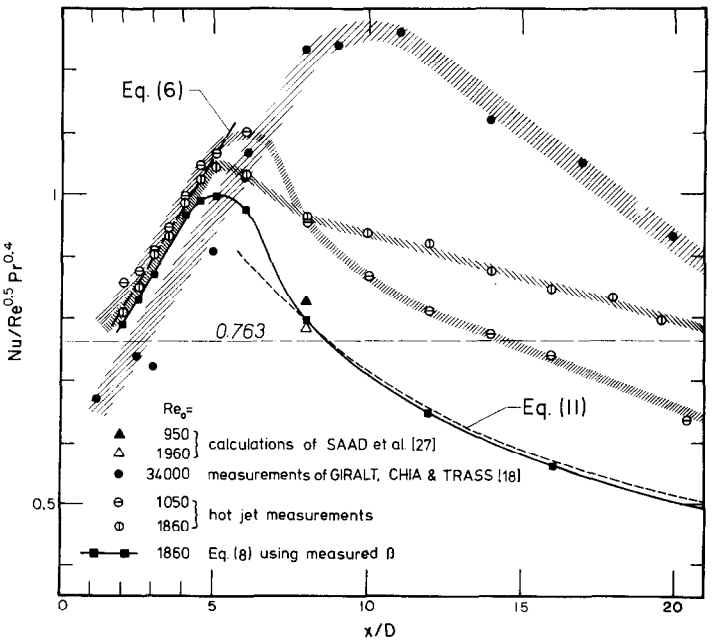

FIG. 13. Heat transfer rate at the stagnation point.

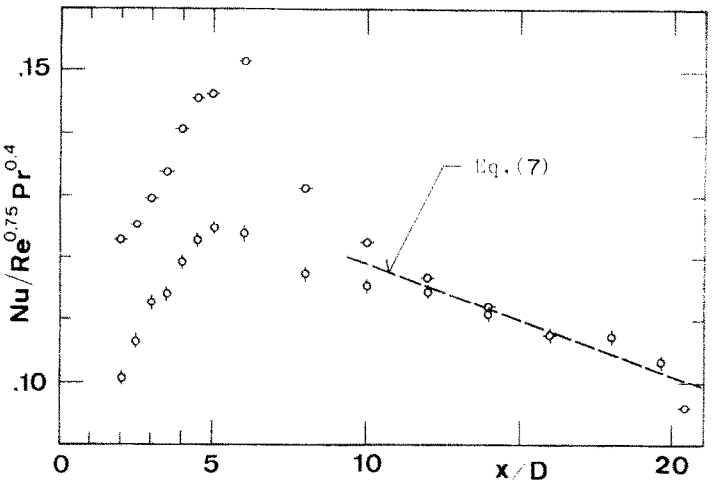

FIG. 14. Turbulent heat transfer rate at the stagnation point: -○—for $Re_o = 1050$; ⌽—for $Re_o = 1860$.

stagnation line on a cylinder in a turbulent cross flow of air ($Pr = 0.71$). It is assumed that the effect of the integral turbulence scale is negligible compared to the effect of the turbulence intensity itself.

Substituting the value $a = Nu/Re^{1/2}\ Pr^{0.4}$ from equation (11) and the constants $b/Pr^{0.4} = 1.94/0.71^{0.4} = 2.22$ and $c/Pr^{0.4} = -2.41/0.71^{0.4} = -2.76$ to equation (12) we obtain

$$Nu/Re^{1/2}\ Pr^{0.4} = 2.37\left(\frac{x + x_0}{D}\right)^{-0.5} + 2.22\left(\frac{Tu\,Re^{1/2}}{100}\right) - 2.76\left(\frac{Tu\,Re^{1/2}}{100}\right)^2 \quad (13)$$

which approximates quite well with the experimental data for the hot jet beyond the distance $x/D \geqslant 8$ and for the cold jet beyond $x/D \geqslant 12$.

Heat transfer radial distribution

The variations of the local heat flux density with the radius, at the nozzle-to-plate distance within $x/D = 2$ to 16 and for the efflux Reynolds number $Re_o = 1860$ are shown in Fig. 15. For large distances these distributions have a bell shape. As the distance is decreased below $x/D = 3.5$ the central maximum disappears giving way to a central minimum. The highest heat flux density (660 Wm^{-2}) was recorded at the radius $r/D = 0.5$ and at the distance $x/D = 2$.

The Nusselt number radial distributions are shown in Fig. 16. At small distances ($x/D \leqslant 8$) and at the radius $r/D = 0.5$ to 0.7 we can notice the characteristic annular 'hump' which was observed at the radiius $r/D = 0.5$ in the cold impingement heat transfer investigations [26 and 33] as an 'inner' peak. This peak is a result of a minimum in the laminar boundary layer

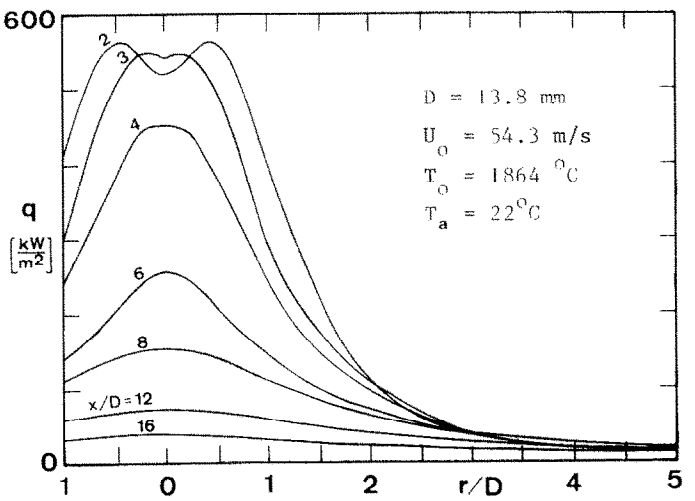

FIG. 15. Heat flux radial distributions on the plate in the impinging round hot gas jet ($Re_o = 1860$).

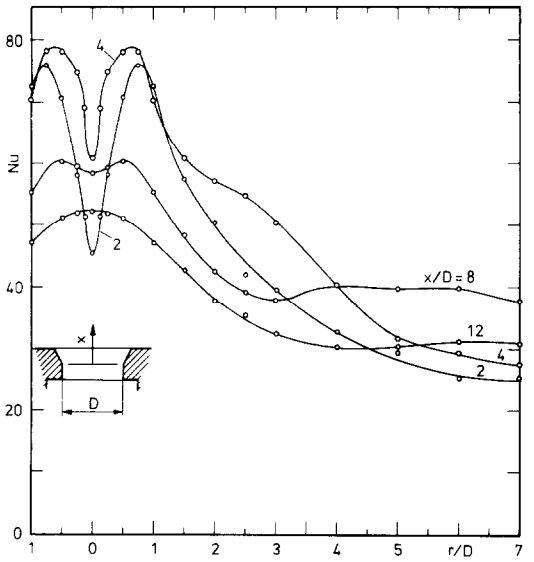

FIG. 16. Radial distributions of the Nusselt number:

$$Nu = \frac{q.D}{(T_{max} - T_w)k}$$

for various distances from the burner nozzle.

thickness caused by the very strong acceleration of the radial flow outside of the boundary layer along the plate which usually appears at this radius and at the small nozzle-to-plate distances for both low and high Reynolds numbers. In spite of the evident turbulent contribution to the heat transfer beyond the distance $x/D = 4$, still at $x/D = 8$ we can observe the minimum on the axis (because of rapid drop of the temperature in a radial wall jet on which the calculation of the heat-transfer coefficient is based). Such slight central minimum at the distance $x/D = 8$ was also observed in the numerical experiment performed by Saad *et al.* [27] with a laminar impinging jet having a flat outlet velocity profile and the Reynolds numbers 950 and 1960.

For the distance $x/D = 4$ at the radius $r/D = 1.6$ we notice the beginning of a small second 'hump' which is shifted outward as the distance x/D increases. This 'hump' may be identified as a transition point of the laminar boundary layer into the fully developed turbulent one and is situated just at an edge of the stagnation region where we have a minus radial gradient of the static pressure (in accord with [18] it is at the radius $r/r_{1/2} \leqslant 2.5$ to 3). It is possible that the stabilizing effect of acceleration produced by the static

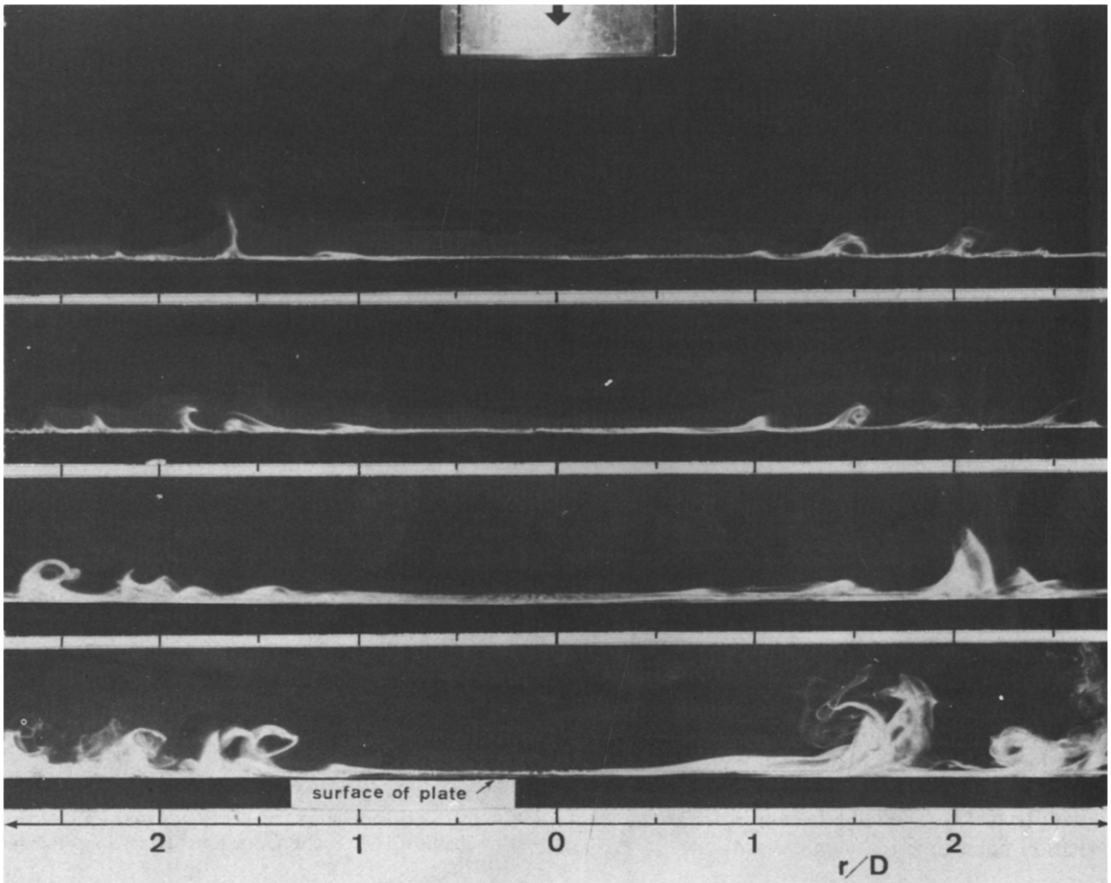

FIG. 17. Flow-visualization in stagnation point region of axisymmetric impinging jet (for $Re_0 = 5 \times 10^3$, $x/D = 1, D = 38.5$ mm).

pressure gradient keeps the boundary layer laminar in the stagnation zone. However beyond the distance $x/D = 4$ at the stagnation point and in its vicinity the laminar boundary layer presumably is interrupted by large scale turbulent eddies periodically generating themselves in a region of a free round jet [15].

Some insight into flow structure in the vicinity of the stagnation point of the impinging jet can be given by a series of flow-visualization pictures obtained with a 'smoke wire' technique [34] and shown in Fig. 17. The jet issued from a long pipe with an efflux Reynolds number of about 5×10^3 and initial turbulence intensity (on the axis) of 3.8%. At the stagnation point and its immediate vicinity the flow along the wall is undisturbed and looks like a laminar one. At the radius about $1D$ we observe a periodic birth of large scale coherent eddies.

4. CONCLUDING REMARKS

The more significant concluding remarks resulting from this experimental investigation are the following:

(1) The mean velocity and temperature profiles at the outlet section of the rapid heating tunnel burner producing the hot jet of combustion products are very similar to turbulent pipe flow profiles and practically are very close to a rectangular form. From LDA turbulence measurements it can be concluded that there is no evidence that additional turbulence is being generated by the combustion phenomena in the tunnel part of the burner.

(2) The axial velocity decay of the hot gas jet submerged in the ambient air with the density ratio $\rho_a/\rho_o = 1$ to 7.6 can be described by the formula using the equivalent diameter $D_e = D(\rho_o/\rho_a)^{1/2}$:

$$U_o/U_x = 6.4\frac{D_e}{x - x_o}$$

which is valid beyond the core length $x/D_e \gtrsim 7$ [35]. The distance of the virtual jet source from the nozzle mouth (x_o) is very sensitive on the flow structure of the jet at the nozzle outlet. For the axial temperature distribution at low distances from the nozzle it is rather hard to establish a simple hyperbolic decay law based on the equivalent diameter.

(3) The heat transfer at the stagnation point can be relatively exactly predicted. Here one may distinguish three heat transfer domains.

(a) The pure laminar layer domain in which due to the strong acceleration effect a laminar boundary layer exists. Within the distances $x/D = 2$ to 4 the result of the heat transfer calculations based on the laminar boundary layer theory given by Sibulkin [29] and measured radial velocity gradients is in a very good agreement with the directly measured data (Fig. 13). The local heat transfer at the stagnation point describes equation (6)

$$Nu = (0.65 + 0.084\, x/D)\ Re^{0.5}\, Pr^{0.4}$$

which is valid for the hot jet ($\rho_a/\rho_o = 7.6$) in the range $x/D = 2$ to 5. For the cold jet ($\rho_a/\rho_o = 1$) in the range $x/D = 1$ to 8.5 in equation (6) we have to use the value 0.57 instead of 0.65. Generally, for the jets with a flat efflux velocity profile this domain extends up to about 1.7 of the core length where we have domination of the very strong laminarizing acceleration effect.

(b) The transient domain, where the radial velocity gradient has its maximum and the turbulence reaching its very high level starts to enhance the convective heat (or mass) transfer.

(c) The turbulent heat transfer domain, where we have a well established turbulence effect. For the investigated hot jet the heat transfer can be described by equation (7) which is valid for $x/D \geqslant 12$ and gives 1.3 to 1.6 times higher values than the laminar boundary layer theory. In order to avoid the limitation of the above equation there is the possibility of using the more universal equation (13) which can be used for both hot and cold jets.

(4) The heat transfer radial distributions in the hot gas impinging jet have a similar characteristic shape as in cold jets at low Reynolds number (below $Re_o = 2500$, [33]. However in the literature there is very scant experimental information about the heat transfer radial distributions in the cold round impinging jets at low Reynolds numbers. At present only some laminar boundary layer theories [36, 37 and 18] or numerical procedures [27] can be used in the immediate vicinity of the stagnation point (up to the boundary layer transition point).

Acknowledgement—The receipt of a one year (1976–77) Research Fellowship from the Delft University of Technology, making most of this work possible is gratefully acknowledged by the first author.

REFERENCES

1. R. B. Smith and T. M. Lowes, Convective heat transfer from impinging tunnel burner flames, Int. Flame Res. Foundation Report, F 35/a/9, Ijmuiden (1974).
2. H. Martin, Heat and mass transfer between impinging gas jets and solid surfaces, *Adv. Heat Transf.* **13**, 1–60 (1977).
3. K. P. Perry, Heat transfer by convection from hot gas jet to a plane surface, *Proc. Inst. Mech. Engrs* **168**, 775–780 (1954).
4. E. H. Comfort, T. J. O'Connor and L. A. Cass, Heat transfer resulting from the normal impingement of a turbulent high temperature jet on an infinitely large plate, *Proc. Heat Transf. Fluid Mech. Inst.* 44–62 (1966).
5. J. A. Fay and F. R. Riddell, Theory of stagnation point heat transfer in dissociated air, *J. Aeronaut. Sci.* **25**, 73–85 (1958).
6. R. N. McBride, Prediction of a convective heating system, 4th Symp. on Flames and Industry, Imperial College, London (1972).
7. C. O. Popiel, A. Kamasa and L. Boguslawski, Traversing mechanism, H. T. Section Ann. Rep., Tech. Univ., Poznań (1976).
8. Aardgas-Basisgegevens over Gronings aardgas. Samengesteld door het beproevings Laboratorium van de n.v. Nederlandse Gasunie (1968/1971).

9. C. O. Popiel and L. Bogusławski, Local heat-transfer coefficients on the rotating disk in still air, *Int. J. Heat Mass Transfer* **18,** 167–170 (1975).
10. D. Bradley and K. J. Matthews, Measurement of high gas temperatures with fine wire thermocouples, *J. Mech. Engng Sci.* **10,** 299–305 (1968).
11. J. H. Kent, A noncatalitic coating for platinum-rhodium thermocouples, *Combust. Flame* **14,** 279–282 (1970).
12. S. Corrsin and M. S. Uberoi, Further experiments on the flow and heat transfer in a heated turbulent air jet, NACA Report 998, 1–17 (1951).
13. H. A. Becker and A. P. G. Brown, Velocity fluctuations in turbulent jets and flames, *12th Symposium on Combustion*, The Combustion Inst., Pittsburgh, pp. 1059–68 (1969).
14. I. Wygnanski and M. Fiedler, Some measurements in the self-preserving jet, *J. Fluid Mech.* **38,** 577–612 (1969).
15. S. C. Crow and F. H. Champagne, Orderly structure in jet turbulence, *J. Fluid Mech.* **48,** 547–591 (1971).
16. C. D. Donaldson and R. S. Snedeker, A study of free jet impingement. Part 1. Mean properties of free and impinging jets, *J. Fluid Mech.* **45,** 281–319 (1971).
17. C. D. Donaldson, R. S. Snedeker and P. D. Margolis, A study of free jet impingement. 2. Free jet turbulent structure and impingement heat transfer, *J. Fluid Mech.* **45,** 477–512 (1971).
18. F. Giralt, C. J. Chia and O. Trass, Characterization of the impingement region in an axisymmetric turbulent jet, *Ind. Engng Chem.* **16,** 21–28 (1977).
19. L. Bogusławski and C. O. Popiel, Flow structure of the round turbulent jet in the initial region, *J. Fluid Mech.* **90,** 531–539 (1979).
20. M. W. Thring and M. P. Newby, Combustion lengths of enclosed turbulent jet flames, *4th Symposium on Combustion*, Baltimore, 789–796 (1953).
21. C. J. Chen and W. Rodi, On decay of vertical buoyant jets in uniform environment, *6th Int. Heat Transfer Conference*, Toronto **1,** 97–102 (1978).
22. P. D. Sunavala, C. Hulse and M. W. Thring, Mixing and combustion in free and enclosed turbulent jet diffusion flames, *Combust. Flame* **1,** 179–193 (1957).
23. R. A. M. Wilson and P. V. Danckwerts, Studies in turbulent mixing – II. A hot air jet. *Chem. Engnng Sci.* **19,** 885–895 (1964).
24. Y. Era and A. Saima, An investigation of impinging jet (experiments by air, hot air and carbon dioxide), *Bull. J.S.M.E.* **19,** 800–807 (1976).
25. E. R. G. Eckert and R. H. Drake, Jr, *Analysis of Heat and Mass Transfer*, p. 432. McGraw-Hill, New York (1972).
26. R. Gardon and J. Cobonque, Heat transfer between a flat plate and jets of air impinging on it, Int. Heat Transfer Conference, Univ. Colorado, Boulder, 454–460 (1961).
27. N. R. Saad, W. J. M. Douglas and A. S. Mujumdar, Prediction of heat transfer under an axisymmetric laminar impinging jet, *Ind. Engng Chem.* **16,** 148–154 (1977).
28. F. Coeuret, Transient de matiere lors de l'impact normal de jets liquides circulaires immerges, *Chem. Engng Sci.* **30,** 1257–1263 (1975).
29. M. Sibulkin, Heat transfer near the forward stagnation point of a body of revolution, *J. Aeronaut. Sci.* **19,** 570–571 (1952).
30. V. Kottke, H. Blenke and K. G. Schmidt, Messung und Berechnung des örtlichen und mittleren Stoffübergangs an stumpf angeströmten Kreisscheiben bei unterschiedlicher Turbulenz, *Wärme Stoffübertragung* **10,** 89–105 (1977).
31. C. J. Hoogendoorn, The effect of turbulence on heat transfer at a stagnation point, *Int. J. Heat Mass Transfer* **20,** 1333–1338 (1977).
32. S. Sikmanovic, S. Oka and S. K. Djurevic, Influence of the structure of turbulent flow on heat transfer from a single cylinder in a cross flow, *Proc. 5th Int. Heat Transf. Conference*, Vol. II, 320–324, AICHE, NY (1974).
33. R. Gardon and J. C. Akfirat, The role of turbulence in determining the heat transfer characteristic of impinging jets, *Int. J. Heat Mass Transfer* **8,** 1261–1272 (1965).
34. C. O. Popiel, An investigation of round impinging jets: The flow-visualization with a 'smoke wire' technique, H. T. Section Ann. Rep., Tech. Univ., Poznań (1978).
35. P. Hrycak, D. T. Lee and J. W. Gauntner, Experimental flow characteristics of a single turbulent jet impinging on a flat plate, NASA T. N. D-5690 (1970).
36. S. P. Kezios, Heat transfer in the flow of a cylindrical air jet normal to an infinite plane, Ph.D. Thesis, Illinois Institute of Technology (1956).
37. C. J. Chia, F. Giralt and D. Trass, Mass transfer in axisymmetric turbulent impinging jets, *Ind. Engng Chem.* **16,** 28–35 (1977).

CONVECTION THERMIQUE SUR UN PLAN FRAPPE PAR UN JET DE GAZ CHAUD A FAIBLE NOMBRE DE REYNOLDS

Résumé—Une étude expérimentale a été faite sur le transfert thermique local pour un plan isotherme et un jet chaud, circulaire l'attaquant normalement, het de produits de combustion sortant à grande vitesse d'un foyer. Différentes sondes sont utilisées pour mesurer le flux thermique, les distributions de vitesse moyenne et de température. Quelques intensités de turbulence sur l'axe sont mesurées avec un anémomètre laser Doppler. Toutes les mesures sont réalisées à deux nombres de Reynolds de sortie égaux à 1860 et 1050; le rapport des densités entre les produits chauds de la combustion et l'air ambiant est 7,6. Le transfert thermique est mesuré à des distances comprises entre 20 et 200. Le transfert thermique au point d'arrêt pour des distances $x/D \leqslant 5$ est en bon accord avec la théorie de la couche limite laminaire de Sibulkin. Dans la région développée $x/D \geqslant 8$, on observe une forte turbulence de jet libre dont les effets augmentent le transfert thermique. Les distributions radiales du transfert thermique sont qualitativement cohérentes avec celles connues dans les études de jet froid incident aux faibles nombres de Reynolds.

KONVEKTIVER WÄRMEÜBERGANG AN EINER PLATTE IN EINEM AUFTREFFENDEN HEIßEN GASSTRAHL BEI KLEINER REYNOLDS-ZAHL

Zusammenfassung—Der lokale Wärmeübergang an einer ebenen isothermen Fläche in einem normal auftreffenden runden, heißen Strahl von Verbrennungsprodukten eines schnell heizenden Tunnelbrenners wurde untersucht. Ein Wärmeleitungseinsatz, Staurohre und feine Drahtthermoelemente wurden für die Messung des Wärmestroms, der mittleren Geschwindigkeit und der Temperaturverteilung verwendet. Einige Messungen der Intensität der relativen Turbulenz an der Mittellinie wurden mit einem Laser-Doppler-Anemometer vorgenommen. Alle Meßergebnisse wurden für zwei Reynolds-Zahlen 1860 und 1050 erhalten. Das Dichteverhältnis zwischen warmen Verbrennungsprodukten und der Umgebungsluft war 7.6. Der Wärmeübergang wurde bei Entfernungen zwischen 2 D und 20 D gemessen. Der Wärmeübergang am Staupunkt innerhalb der Entfernung $x/D \leqslant 5$ stimmt gut mit der laminaren Grenzschichttheorie von Sibulkin überein. Im ausgebildeten Bereich $x/D \geqslant 8$ wurden starke Turbulenzeffekte im Freistrahl beobachtet, die den konvektiven Wärmeübergang verstärken. Die radialen Verteilungen des Wärmeübergangs befinden sich qualitative in Übereinstimmung mit den aus Untersuchungen an kalten Freistrahlen kleiner Reynolds-Zahlen bekannten Verläufen.

КОНВЕКТИВНЫЙ ТЕПЛОПЕРЕНОС НА ПЛАСТИНЕ ПРИ НАТЕКАНИИ КРУГЛОЙ СТРУИ НАГРЕТОГО ГАЗА С НИЗКИМ ЧИСЛОМ РЕЙНОЛЬДСА

Аннотация — Экспериментально исследовался локальный теплоперенос на плоской изотермической поверхности при натекании на нее под прямым углом из туннельной горелки круглой нагретой струи, содержащей продукты горения. Для измерения распределений плотности теплового потока, средней скорости и температуры использовались теплопроводная вилка, трубки Пито и проволочные термоэлементы. С помощью лазерного допплеровского анемометра проведены измерения относительной интенсивности аксиальной турбулентности. Все измерения проводились при значениях числа Рейнольдса истечения струи, равных 1860 и 1050; отношение плотности продуктов горения к плотности окружающего воздуха составляло 7,6. Плотность теплового потока измерялась на расстояниях от $2D$ до $20D$. Измеренное значение плотности теплового потока в точке торможения на расстоянии $x/D \leq 5$ хорошо согласуется со значением, рассчитанным по теории ламинарного пограничного слоя Сибулькина. В области развитого течения, $x/D \geq 8$, наблюдалась сильная свободная турбулентность струи, способствующая интенсификации конвективного теплопереноса. Радиальное распределение плотности теплового потока согласуется количественно с известными значениями, полученными при исследовании натекающей холодной струи при низких значениях числа Рейнольдса.